N71-35620

NASA TECHNICAL MEMORANDUM

NASA TM X-67930

NASA TM X-67930

CASE FILE

OPTICAL TRANSMITTANCE OF FUSED SILICA AT ELEVATED TEMPERATURES DURING HIGH ENERGY ELECTRON BOMBARDMENT

by Albert B. Smith
Lewis Research Center
Cleveland, Ohio

OPTICAL TRANSMITTANCE OF FUSED SILICA AT ELEVATED TEMPERATURES DURING HIGH ENERGY ELECTRON BOMBARDMENT

Albert B. Smith
Lewis Research Center
National Aeronautics and Space Administration
Cleveland, Ohio

Abstract

An experimental determination of the optical transmission of Corning 7940 UV and Suprasil I fused silica has been made. The LeRC dynamitron provided the equivalent ionizing radiation and high temperature that the transparent gas divider of an operating nuclear light bulb engine would experience. The irradiation induced absorption was measured at 2150 Å, 2700 Å, and 4500 Å. The length of the irradiations were sufficient so that an equilibrium between radiation induced coloration and high temperature annealing was reached. The experimental results indicate a significant optical absorption, particularly at the shorter wavelength, which would make the use of fused silica in this concept questionable.

Introduction

One interesting nuclear propulsion concept is the gaseous core nuclear reactor. In one design fused silica is proposed as a transparent wall separating the fuel and the propellant. This Nuclear Light Bulb transfers the energy of the fissioning fuel by thermal radiation through the fused silica to a hydrogen propellant seeded with opaque particles. The radiant energy absorbed lies in the range of 2000 Å to 10 000 Å.

Practical realization of this propulsion scheme depends in large measure upon the transparency of these cooled fused silica walls at these wavelengths, since the energy must radiate through them. The objective of the present work is to measure under simulated reactor environment, at the wavelengths of interest, the optical transmission of fused silica.

During reactor operation, the fused silica will be exposed to a large flux of fast neutrons and gamma rays emanating from the fissioning fuel it surrounds. Therefore, color centers on optically absorbing centers can be generated as a result of the ionization and damage in the wall material; with subsequent transmission loss. The center of the most prominent irradiation-induced absorption band in the fused silica occurs at a wavelength of 2150 Å. A subsidiary peak occurs at 2700 Å. Additional measurements were made at 4500 Å to determine the width of the absorption band and to check absorption where strong absorption bands are not expected to exist.

These radiation-induced absorption centers are stable at room temperatures, but at elevated temperatures they may be effectively annihilated, annealed or bleached. In this experimental work, and in the application of the nuclear rocket the fused silica will be at temperatures of 600° C to 1000° C. So we have two competing processes affecting the transmission: first, coloration induced by nuclear radiation; and second, annealing of coloration by exposure to elevated temperature. This equilibrium transmission must be sufficiently high for the concept to be workable, and its meas-urement is the prime objective of this experiment.

The Lewis Research Center Dynamitron is used to give an electron beam in which the ionizing dose rate is equivalent to an operating full-scale NLB engine. This accelerator provided 1.5 MeV electrons at current densities in the range of 20 to 150 $\mu A/cm^2$. This corresponds to an ionizing dose rate of 2.0 to 10 Mrad/sec deposited in the specimen, which exceeds anything available in any existing test reactor known today. It was also possible to run for times comparable to the 1000 sec duration of the full scale engine.

Specimen temperature was governed by electron beam heating; most irradiations were done at 80 to 150 $\mu A/cm^2$ current densities to be at the temperature range of interest (600° to 900° C).

A dual beam ratio recording spectrophotometer was designed and used for the measurement of the optical transmission. Samples of Corning Grade 7940 UV, and Suprasil (Amersil Inc.) were tested. These samples of fused silica were chosen because of their high purity, structural integrity, resistance to radiation damage, transparency over a wide range of wavelengths and thermal properties.

Experimental Arrangement

Lewis Dynamitron Electron Accelerator

The LeRC Dynamitron Electron Accelerator is a potential drop accelerator capable of supplying accelerating potentials between 0.3 to 3.0 MeV with voltage stability greater than 99.9 percent.[1] The accelerator can provide direct current, monoenergetic electrons or positive ion beams controllable from 1 μA to 3 mA. In the electron mode of operation a hot tungsten filament is used as a source of particles.

The beam transport system consists of an analyzing magnet, positioning coils and a three element quadrupole focussing set. All power supplies for this system have sufficient stability so that the beam position changes at the output ports are less than 0.1 percent for a monoenergetic beam.

The alignment and focussing of the beam could be monitored by a beam profile monitor and also a closed circuit television system.

Xenon Lamp Source and Supply

A 1000 W Xenon arc lamp was used as the primary light source. The Xenon arc was maintained by a power supply which was continuously variable and monitored to insure lamp performance. This power supply provided dc regulation to ±1 percent with ±10 percent change in line voltage. A fast acting control circuit compensates for changes within the lamp and produces maximum arc stability. The current ripple was 1 percent rms.

TM X-67930

Dual Beam Ratio Recording Spectrophotometer

A large dual beam ratio recording spectrometer was designed and built to measure the transmission through the fused silica samples. This system employed two optical beams, a sample beam and a reference beam. The two beams obtained from a single light source, are separated by using a rotating mirror beam chopper which alternately passes light to the sample mirror or the reference path. Thus the two paths are parallel and separated by approximately 45.72 cm. The beams are collimated to a diameter of 0.72 cm. The sample and the reference light beams are directed at right angles through the faces of the test and reference specimens respectively. The two beam paths are equal in length. They are combined by a serrated surface mirror at the entrance slit of the monochromator. A block diagram of the optical set-up is pictured in Fig. 1. The rotating mirror beam chopper sequentially modulates the sample and reference beams so that locked-in signal processing techniques and phase sensitive detection is possible. The modulating frequency is 13 Hz, and the reference voltage obtained from the rotating mirror triggers the lock in amplifier. Only the modulation component of the detection signal is rectified to produce a dc output from the instrument. In this way, we discriminated against the noise sources such as sample fluorescence, ambient room light, Xenon lamp fluctuations or any remaining Bremsstrahling radiation, and are able to read an extremely weak signal while at the same time ignoring this large background of noise.

The monochromator could select a particular wavelength range is between 160 and 3500 millimicrons. Since both sample and reference beams have common detection and amplifier components and ratio recording (or the comparison of sample beam intensity with reference beam intensity was used) inaccuracies due to amplifier gain or spectral response of the photomultiplier is eliminated.

Optical Base

The Xenon lamp, monochromator, mirrors and beam splitters, reference path furnace and specimen holder box were all securely fastened to a (91.4 cm wide) × (182.9 cm long) × (3.82 cm deep) aluminum table with a top surfaced machined flat to 0.050 mm. Since all these parts are held in their relative positions, the whole base could be moved without disturbing the critical beam alignment. The complete system was then suspended from the ceiling by unistruts to completely isolate it from any vibrations caused by the vacuum pumps on the electron-beam transport system.

Electronic System

The control panel containing the phase-sensitive amplifier and the remaining electronic equipment was located in the dymanitron control room located out of the irradiation area and separated by 30.5 m. The detection system included a 4 pen chart recorder which simultaneously recorded furnace temperature, specimen temperature, specimen holder temperature, and the amplified ratio between specimen and reference beams. Readout of the wavelengths and actual position of the electron beam on the specimen was accomplished by closed circuit television camera remotely con-

trolled from the dynamitron control console. These were monitored continuously while the test was being run. The output of the phase-sensitive amplifier was checked by viewing the signal and the rectified signal on a dual oscilloscope.

The photomultiplier tube was shielded by several lead blocks to minimize the noise generated by X-rays present during the irradiations. Since the signal cables were so long low capacity cables were used and a line matching driver amplifier was connected after the pre-amplifier to prevent signal loss.

This system was capable of measurement of optical transmission with an accuracy of ± 1 percent. Response time was limited by the chart recorders which was approximately 1 sec.

Specimen Configuration

The specimen configuration for this experiment was a compromise which met the various requirements of the test. It was sized so that the correct electron energy deposited in the specimen would give the necessary ionizing dose rates. The specimen was thick enough to allow for accurate measurement of the optical transmission for absorption coefficient from 0.05 cm^{-1} to 20 cm^{-1}. The optical path through it was normal to its surface to minimize the effects of thermally induced refractive index gradients, and possible temperature induced stresses which might lead to erroneous transmission determination. The specimens were of wafer form 2.54 cm square and 1.5 mm thick. They were polished flat to 1/4 wavelength of Sodium light and parallel to 2 wavelengths. The specimen was at right angles with respect to the optical beam axis and $20°$ with respect to the electron beam axis.

Specimen Holder

The specimen is held in a metal picture frame type clamp. Figure 2 shows the specimen with the chromel-alumel thermocouple embedded in it and the thermocouple spot-welded to the holder. The thermocouple was wedged tight at the center of the sample by using a tapered hole through the fused silica. Spring tension of its leads and thermo expansion of the thermocouple ball tended to secure its position throughout the test. The frame type clamp allowed the sample to be held rigidly or a ceramic gasket material could be inserted between the metal holder and the fused quartz for stress free mounting. The holder also provided cooling slits which blew a sheet of Helium across the faces of the specimen. At the same time cooling gas was directed against the aluminum foil through which the electrons passed. The foil holder was also cooled by water jackets and the gas cooling could be omitted if desired. This double cooling method could be used when very high machine currents were used. Each cooling line was valved and adjustable. The whole specimen holder assembly, which included the cooling tubes, thermocouples, and thermocouple connectors and fittings, was removable from the sample box. It was grounded to the system to help prevent any charge buildup, repeatable positioning of the specimen was guaranteed by eight bolt holes and a centering edge. Readout of the remotely operated upstream beam stop and the thermocouples was con-

stantly recorded during the experiment.

Sample Box

The specimen was inserted in the holder and then the holder bolted to the sample box. The box provided whatever environment was necessary air, helium or vacuum, for the specimen under test. It was connected directly to the beam transport tube and therefore included the aluminum foil (approximately 0.05 mm thick). In this way, the Dynamitron vacuum was not affected by the environment used in the test. The sample box also provided collimation for the optical light beam before and after the specimen. It could be sealed by using SiO_2 end windows. Permanent magnets were used to prevent the windows from being darkened. It was possible to see the specimen during the experiment by remote television camera through another SiO_2 port directly inline with the 20° electron beam line.

Therefore, specimen luminescence could be visually observed, and by using a ZnS coating on the aluminum foil, the beam spot could be continually monitored throughout the experiment. Any beam wandering could be instantly seen. In addition the size and position of the beam spot was determined by a separate test using PVC plastic indicators at the positions of the Al window sample and the Faraday cup. This was done as a standard procedure before each test run.

Calibration

Calibration of the electron beam striking the specimen was done by removing the fused silica holder and inserting a water-cooled or air-cooled Faraday cup. The Faraday cup was positioned exactly the same as the specimen and held by the same eight bolts. It had a guard ring to prevent erroneous contributions from any scattered secondary electrons. In this way external beam current hitting the specimen was calibrated against the internal machine beam current and dial setting.

Absorption Data Analysis

The 4 channel Bristol recorder simultaneously records specimen temperature T_s, ambient or furnace (reference path) temperature, T_F, holder temperature T_H, and the ratio of the specimen to reference signals as a function of elapsed time, t. These two signals which constitute the output of the phase sensitive detector, are proportional to the intensity of the sample and reference beams. Thus a record of relative transmission and temperature during the electron irradiation is accomplished. If a single test specimen only was used, the light transmitted I, through its flat, parallel faces is a fraction of the incident light I_o given by I/I_o. This fraction represents the light lost through absorption and reflection if interference effects are ignored. For a specimen of thickness ℓ, the fraction lost through absorption is of the form $e^{-\alpha\ell}$. Multiple reflections in the specimen at the glass-air interface effects the total transmitted intensity. The light transmitted through the first face is $I_o e^{-\alpha\ell}(1 - r)$ and $I_o e^{-\alpha\ell}(1 - r)^2$ through the second face.

The total transmitted intensity may be

summed[2,3] and expressed as:

$$I = I_o e^{-\alpha\ell} (1 - r)^2 \left[1 - (e^{-\alpha\ell})^2 r^2\right]^{-1} \quad (1)$$

or

$$\frac{I}{I_o} = \frac{e^{-\alpha\ell} (1 - r)^2}{\left[1 - (e^{-\alpha\ell})^2 r^2\right]} \quad (2)$$

where α is the absorption coefficient at a particular wavelength, r is the reflection loss, and is related to the index of refraction n by the relation:

$$r = \left(\frac{n - 1}{n + 1}\right)^2 \quad (3)$$

For fused silica, in the wavelength range we are considering, n does not exceed 1.6^4 and hence the denominator of Eq. (2) is essentially (1) assuming the no absorption case where $e^{-\alpha\ell} = 1$ so that multiple reflections can be safety ignored. So the reflection loss is just $(1 - r)^2$, and we may write:

$$\frac{I}{I_o} = (1 - r)^2 e^{-\alpha\ell} \quad (4)$$

or

$$\alpha = -\frac{1}{\ell} \left[\left(\ln \frac{I}{I_o}\right) - \ln(1 - r)^2\right] \quad (5)$$

In this experiment a reference specimen was provided of the exact same composition as the test sample, in the axial crusilite vacuum furnace of the reference optical path. This technique effectively cancels reflection losses so that Eq. (5) reduces to simply:

$$\alpha = -\frac{1}{\ell} \ln \frac{I(\lambda,\dot{D},t,T)}{I_o(\lambda)} \quad (6)$$

where $I_o(\lambda)$ is the chart recorder amplitude before the electron beam is turned on and $I(\lambda,\dot{D},t,T)$ the recorder amplitude at a time t, after the beam is on.

The raw data from the recorder strip chart of optical transmission, specimen temperature, and electron current density or ionizing dose rate are presented as the electron irradiation history of each specimen by converting the optical transmission to radiation induced absorption coefficient (by use of eq. (6)) and graphing these parameters as a function of elapsed time. Typical raw data is shown in Fig. 3, in this case for a wavelength of 2700 Å and a specimen 1.5 mm thick of Suprasil I.

A useful computational scheme devised by Burrel, Wright, and Watts[5] is used to calculate the ionizing dose rate through the specimens. This semi-empirical technique is based on the Monte Carlo electron energy transfer data of Berger.[6] Using this technique, an approximate result is calculated for the complex relation between the ionizing dose rate, $\dot{D}$, and the electron current density, J, for an electron of kinetic energy, E, of 1.5 MeV impinging upon the specimen configuration used in this experiment. This

technique is described in the appendix. The results are now discussed.

The ionizing dose rate is $\dot{D} = 0.13$ D (krad/sec). Because of the complexity of the atomic processes involved in determining the ionizing dose rate, an error of ±25 percent is estimated. A full-scale NLB engine operating at a radiating temperature of 15000° R is expected to give an ionizing dose rate of 5.4×10^6 R/sec.[7] This dose rate is well within the current capability of the Lewis Dynamitron Electron Accelerator.

Specimen temperature was by electron beam heating, and most irradiations were done at 80 to 150 μA/cm² current densities. Helium cooling gas was also employed at times so that the specimen temperature was controllable in the range of interest (600 to 900 C). Satisfactory temperature measurement using the chromel-alumel thermocouples embedded in the sample, and the sample holder, had error less than ±20° C based on the inherent accuracy of measuring equipment and the electron beam hitting the thermocouple. Since the designed spectrophotometer was capable of optical transmission measurement under laboratory conditions of ±1 percent, this gives a measurement accuracy of about ±16 percent at all the induced absorption coefficients of between 1.0 cm⁻¹ and 12 cm⁻¹.

Figure 4 presents the electron irradiation history of a 1.5 mm Surpasil I specimen at 2150 Å. Here the ionizing dose rate is raised in step intervals. It can be seen that both the temperature and the absorption coefficient is increased correspondingly and that the temperature does lie in the range of interest.

There is a slow decrease in this absorption coefficient in time at this temperature. Generally, the induced absorption coefficient is decreased very slightly from its initial value at the outset of the irradiation but does not go to very low values until the bombardment is stopped.

Although 2150 Å is the wavelength of primary interest, the temporal behavior at two other wavelengths was investigated, namely at 2700 Å and 4500 Å. The curves are shown in Figs. 5 and 6. The curves of the ionizing dose rate, temperature, and induced absorption coefficient of the Suprasil I specimen are very similar to those exhibited by the Corning 7940 UV specimens. Plateaus of these parameters seem to follow the level of the dose rate employed, with no real decay of the absorption coefficient as the temperature is increased by increased irradiation dose.

The results of the optical transmission of a Suprasil I specimen during irradiation at wavelengths of a 4500 Å are presented in Fig. 6. It is expected that this curve would be different than those at the previous wavelengths since Corning 7940 UV and Suprasil I fused silica does not have any strong irradiation-induced absorption bands at the 4500 Å wavelength. Accordingly, it is no surprise to see at a steady state dose rate with a steady temperature of 400° C maintained that the induced absorption coefficient shows a sharp rise and then decays rapidly to a steady lower value until the beam is shut off. The curious bump in the induced absorption curve at the end of the run is due to a sudden burst of electrons from the

dynamitron during a spark out. The trends, however, for both the fused silica samples are similar. There was some question as to whether heating the specimen by the elctron beam could produce an apparent loss of optical transmission by stresses in the specimen which thereby displace the optical beam off the monochromator slit. In order to test this possibility of a thermal effect erroneously giving a loss in optical transmission, tests were run at 3000 Å, a wavelength at which the induced absorption was negligible. Three runs were made using 1.5 mm samples of Corning 7940 UV fused silica. One test was performed in open air, and one with the sample box evacuated, and one with Helium.

The results clearly show there was no anomaly due to specimen temperature even though very high temperatures were reached by the test sample.

A Corning 7940 UV specimen was soft mounted using a special ceramic material in order to remove any doubt that thermal strains imposed by the sample holder might give erroneous results. The wavelength of the test is 2150 Å, and no significant difference in the results are evident using this ceramic soft mounting material. All parameter trends are repeated and verified.

The steady-state irradiation-induced absorption coefficient at 2150 Å over temperatures ranging from 100° to 1000° C are plotted against the ionizing dose rate in Fig. 7. Also shown in Fig. 7 are curves from steady-state irradiations obtained recently from the experiments conducted by Palma and Gagosz in Ref. 8. It is apparent from these curves and data points that there is evidence of disagreement in these two experiments. The claim of Palma and Gagosz that the induced absorption coefficient at a given temperature first rises with increasing dose rate, reaches a maximum value, and then begins to decrease with increasing dose rate is not verified by this experimental work. Although this work has been done with specimens of the same size, composition and configuration, the results, as presented by this graph, differ markedly. A thourough examination of their apparatus has failed to reveal to us the cause of this discrepancy.

Discussion and Conclusions

This experimental study attempted to determine the level of the irradiation-induced absorption expected in the transparent wall of the nuclear light bulb engine (NLB) when the wall is kept at elevated temperatures. The data pertaining to the optical transmission of Corning 7940 UV and Suprasil I fused silica verified the behavior of the induced absorption coefficient as follows:

In irradiations conducted at 2150 Å, the wavelength of primary interest, the irradiation-induced absorption coefficient reached a steady state value once the specimen temperature had reached equilibrium.

Increasing the specimen temperature by raising the electron current density or ionizing dose rate caused the induced absorption coefficient to rise to a higher steady state value.

Increasing the temperature of the specimen

4

while maintaining the same ionizing dose rate resulted in a lower value for the irradiation-induced absorption coefficient to a lower steady state value.

The irradiation-induced absorption coefficient decreased rapidly after the electron beam was shut down, although sometimes after reaching a minimum value there would be a small increase or hump present caused by the response of the recorder. This investigation proved that Corning 7940 UV and Suprasil I at the wavelengths of 2150 Å, 2700 Å and 4500 Å are approximately the same, with no significant differences between these two materials in effects of temperature or irradiation.

Values ranging from 14.5 cm^{-1} to 2.2 cm^{-1} were recorded for the irradiation-induced absorption coefficient at the wavelength of 2150 Å depending upon the test conditions.

At the wavelength of 2700 Å both types of specimens exhibited essentially the same behavior as stated above at 2150 Å. The induced absorption coefficient varied between 3 cm^{-1} to 9.7 cm^{-1} depending on the test conditions.

The response at the 4500 Å wavelength displayed less transmission loss than at the wavelengths 2700 Å or 2150 Å as expected. In addition the induced absorption coefficient rose to a maximum value and then decayed rapidly to a lower equilibrium value. This transient change in transmission was expected since the ultra-pure fused silica used does not exhibit any strong absorption bands at 4500 Å.

No anomalous loss of optical transmission was recorded due to the extremely high temperatures experienced by the specimens regardless of whether the specimen environment was air, air-helium gas mixture, or a vacuum. Using a special ceramic gasket material as a soft mount for the fused silica did not alter the results. Measurements of the induced absorption coefficient when the specimen was soft mounted indicated the same trends and almost the identical loss of transmission at the wavelength of 2150 Å as the firm mounted specimen. These two results show no erroneous results due to thermal stresses caused by the original firm mounting of the specimen which had any significant effect on the optical transmission at this important wavelength.

This particular investigation does not give a complete answer as to the practical realization of the nuclear light bulb propulsion scheme. An extension of this study to include the effects of optical bleaching, absorption in the vacuum ultraviolet wavelength region, wavelength scans over the range of 2000 Å to 3000 Å, additional test for any anomaly due to high temperature, and the temporal behavior and measurements of the irradiation-induced optical absorption of other promising transparent wall materials such as aluminum oxide, beryllium oxide and titanium oxide should be performed. Since the objective of the present investigation was to measure under simulated reactor environment, at the wavelengths of interest, the optical transmission of fused silica, it is desirable to simulate the actual test conditions as accurately as possible. Therefore, it would be advantageous to extend this work also by utilizing a high energy proton beam which would

simulate neutron damage in the specimen. Although there are still areas, as shown above, needing attention in this work, the results of the present investigation indicates significant optical absorption at the wavelengths of interest. This conclusion implies that the feasibility of this concept insofar as it depends upon fused silica transparency under these conditions, is open to question.

Appendix - The Calculation of Electron Dose Rates In Thick Specimens

Determining the ionizing dose rate due to the penetration of relativistic electrons into specimens which are thick compared to the range of the electron is made more complex because of the inelastic scattering and straggling of the electron energy. The electron traverses along a zig-zag path due to the inelastic scattering. These two effects result in a broad distribution of electron energy loss. If the energy loss is averaged over this broad distribution, the energy in the deposited specimen can be calculated and converted to ionizing dose rate. The useful computational scheme of Burrel, Wright and Watts[5] which is in part based on the Monte Carlo electron transfer data of Berger[6] is used in this report and by Palma and Gagosz[7] in their similar work on fused silica. To obtain a sufficient dose rate, it is required that the fraction of the incident electron energy deposited be as large as possible, but it is necessary to trade off this parameter with the fraction of the incident electrons actually stopping in the specimen (keeping this to a minimum so that the charge buildup in the specimen will be small). Burrel, et al[5] obtain expressions for the fractions above by fitting the data of Berger[6] and yield the equation below for normal incidence:

$$p(\ell,\theta) = 0.45\left[1-\exp(-0.653\ z - 2.40\ z^2 - 6.89\ z^3)\right]$$
(1)

$$n(\ell,\theta)=0.912\left[1-\exp(-0.0512\ z + 1.128\ z^2 - 9.38\ z^3)\right]$$
(2)

where:

$n(\ell,\theta)$ = Fraction of the incident electron energy deposited

$p(\ell,\theta)$ = Fraction of the incident electrons absorbed in the specimen

θ = Electron angle of incidence with the specimen surface

also

$$z = \frac{\ell}{x_0}$$
(3)

where z represents the fraction of the average path length x_0 traversed by the electron in penetrating the distance ℓ. This ratio plotted against the sum of the reflection and transmission factors of Berger show little change with variation in electron energy.

The relationship between the average path length x_0 and the extrapolated range $R(E)$ is approximated by:

$$z = \frac{\ell}{(1.33 - 0.19\,E)R(E)} \qquad (4)$$

where:

ℓ = specimen thickness (cm)

E = electron kinetic energy (MeV)

R(E) = electron range (cm)

With these considerations in mind, the specimen thickness ℓ, was chosen as 1.5 mm. This value permits accurate determination of the optical transmission. The range of 1.5 MeV electron in fused silica is R(E) = 4 mm therefore z is 0.36, and $p(\ell,\theta)$ = 0.54 and $n(\ell,\theta)$ = 0.25. Therefore, 25 percent of the penetrating electrons are absorbed giving up 54 percent of their energy in a fused silica sample 1.5 mm thick. The extreme complexity of the processes involved makes the relation between the ionizing dose rate $\dot{D}$ and the electron density J at a kinetic energy of 1.5 MeV only an approximation. The relation using the technique described above is the same one used by Palma and Gagosz[7] and is expressed as:

$$\dot{D} = p(\ell,\theta)\left(\frac{JE}{\rho\ell}\right)\left[1 + \tan\beta\left(\frac{\ell}{\omega}\right.\right.$$
$$\left.\left. + \frac{1}{3}\frac{\ell^2}{\omega^2}\tan\beta\right)\right]^{-1} \times 10^5\,\frac{RAD}{SEC} \qquad (5)$$

Substituting the values given below into Eq. (5) where

$p(\ell,\theta)$ = 0.54, ρ, the density of fused silica is given as 2.2 gm/cm^2 with a specimen thickness ℓ of 0.15 cm at the electron beam radius ω.

of 0.5 cm and with β the electron beam angle of divergence for fused silica of approximately $60°$, Eq. (5) numerically reduces to D $\cong$ 0.13J M_{RAD}/sec as mentioned previously.

References

1. Cleland, M. R. and Farrell, P., "Dynamitrons of the Future," IEEE Transactions on Nuclear Science, Vol. 12, No. 3, June 1965, pp. 227-234.

2. Edwards, O. J , "Optical Transmittance of Fused Silica at Elevated Temperatures," Journal of the Optical Society of America, Vol. 56, No. 10, Oct. 1966, pp. 1314-1319.

3. Edwards, O. J., "Optical Absorption Coefficients of Fused Silica in the Wavelength Range 0.17 to 3.5 Microns From Room Temperature to 980° C," TN D-3257, 1966, NASA, Cleveland, Ohio.

4. Anon., "Corning Fused Silica Code 7940," Data Sheet, 1964, Corning Glass Works, Corning, N.Y.

5. Burrell, M. O., Wright, J. J., and Watts, J. W., Jr., "The Calculation of Electron and Bremsstrahlung Dose Rates," Protection Against Space Radiation, SP-169, 1968, NASA, Washington, D.C., pp. 529-538.

6. Berger, M. J., "Transmission and Reflection of Electrons by Aluminum Foils," TN-187, Apr. 1963, National Bureau of Standard, Washington, D.C.

7. Palma, G. E. and Gagosz, R. M., "Optical Absorption in Fused Silica During Irradiation at High-Temperature. H-930709-1, NASA CR-107838, Nov. 1969, United Aircraft Corp., East Hartford, Conn.

8. Palma, G. E. and Gagosz, R. M., "Optical Absorption in Transparent Materials During 1.5 MeV Electron Irradiation," J-990929-1, NASA CR-110907, Oct. 1970, United Aircraft Corp., East Hartford, Conn.
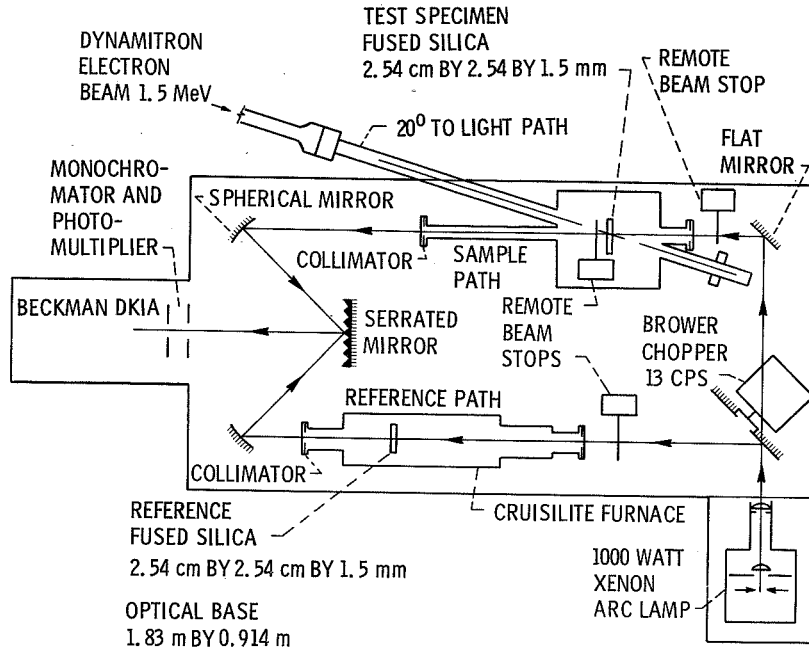
DYNAMITRON
ELECTRON
BEAM 1.5 MeV

TEST SPECIMEN
FUSED SILICA
2.54 cm BY 2.54 BY 1.5 mm

REMOTE
BEAM STOP

20° TO LIGHT PATH

FLAT
MIRROR

MONOCHRO-
MATOR AND
PHOTO-
MULTIPLIER

SPHERICAL MIRROR

COLLIMATOR

SAMPLE
PATH

BECKMAN DKIA

SERRATED
MIRROR

REMOTE
BEAM
STOPS

BROWER
CHOPPER
13 CPS

REFERENCE PATH

COLLIMATOR

CRUISILITE FURNACE

REFERENCE
FUSED SILICA
2.54 cm BY 2.54 cm BY 1.5 mm

1000 WATT
XENON
ARC LAMP

OPTICAL BASE
1.83 m BY 0.914 m

Figure 1. - Diagram of optical reference-sample paths.
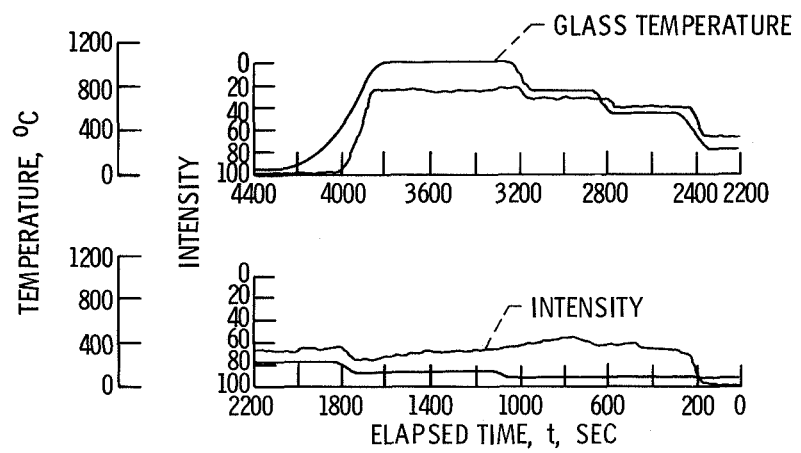

C-70-942
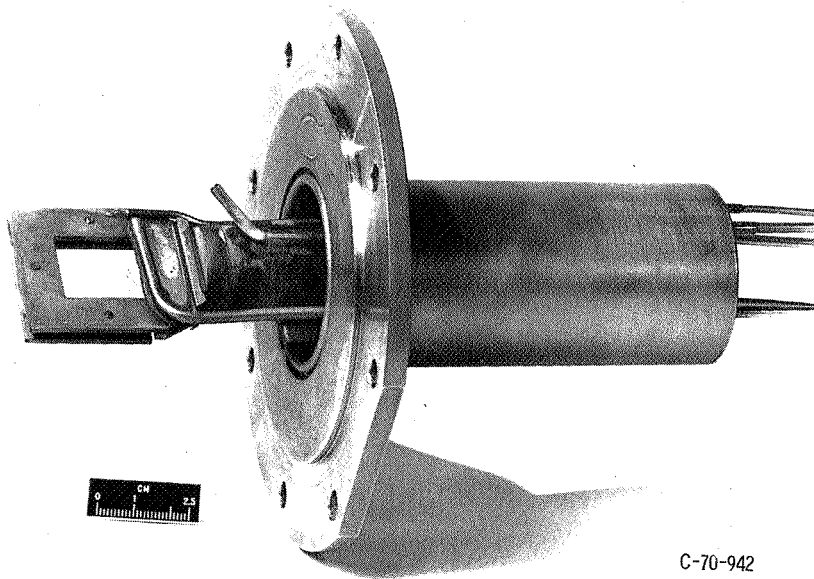
Figure 2. - Specimen holder.

Figure 3. – Typical raw data. (Suprasil I, 1.5 mm thick specimen at 2700 Å).
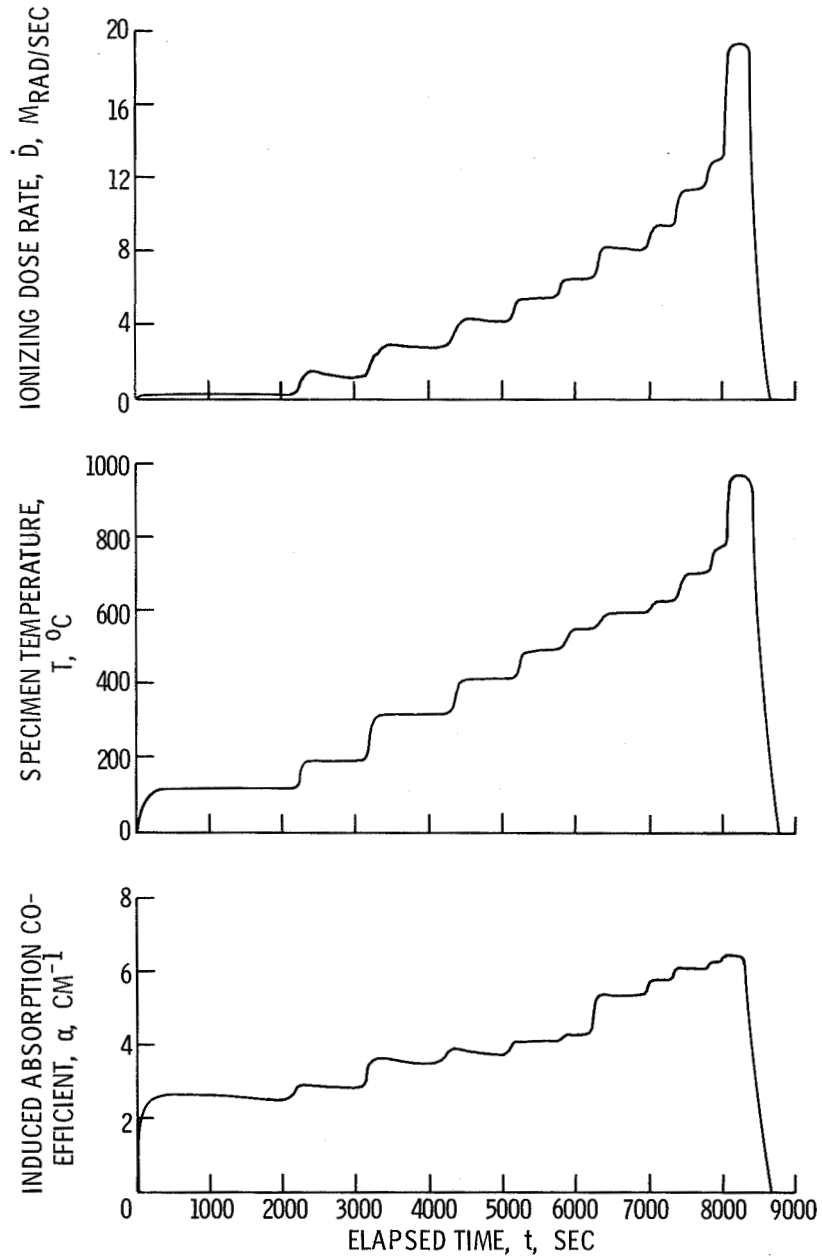
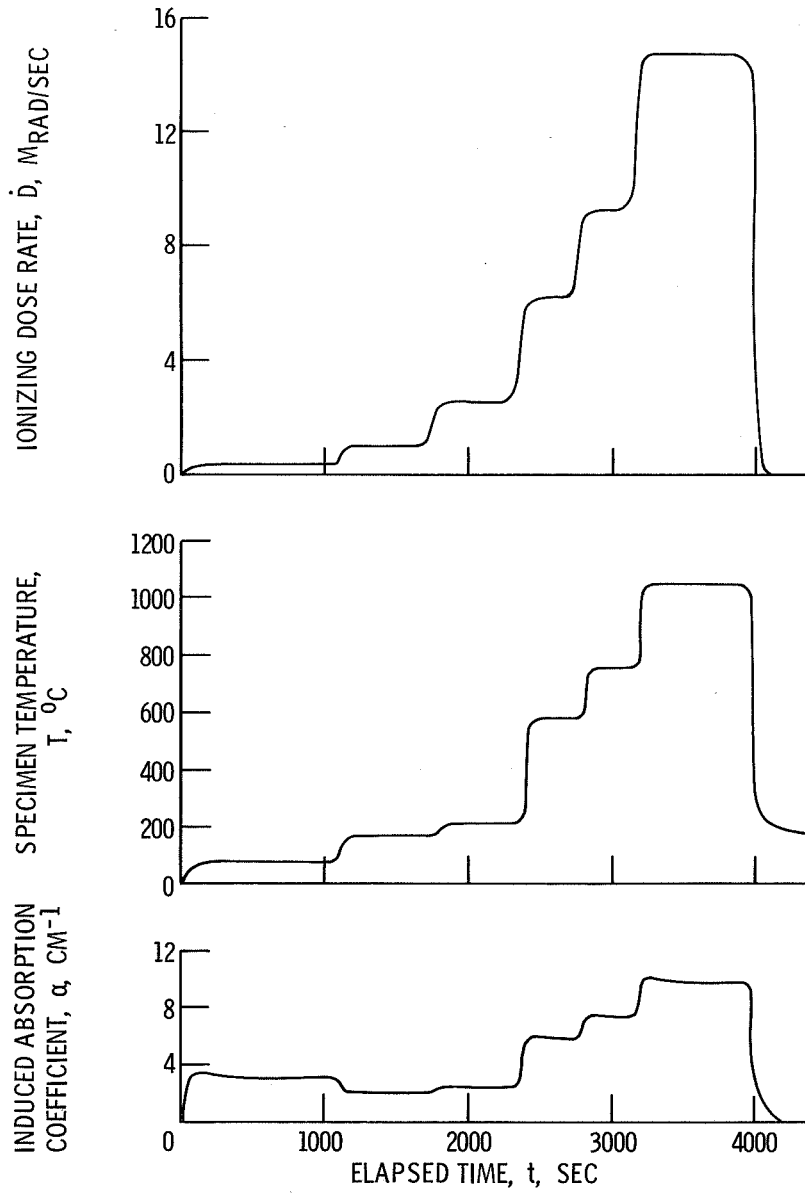Figure 4. - Electron irradiation history of 1.5 mm Suprasil I specimen at 2150 Å.

Figure 5. - Electron irradiation history of 1.5 mm, Suprasil I specimen at 2700 Å.

SPECIMEN TEMPERATURE, °C

	°C
○	100
△	200
□	300
▷	400
●	500
◇	600
▷	700
□	800
◇	900
◇	1000
△	1100

SOLID CURVES FROM UNITED AIRCRAFT RESEARCH LABORATORIES REPORT J 990929-1

LeRC DATA

UAC DATA

INDUCED ABSORPTION COEFFICIENT, α, cm^{-1}

IONIZING DOSE RATE, $\dot{D}$, M$_{RAD}$/SEC
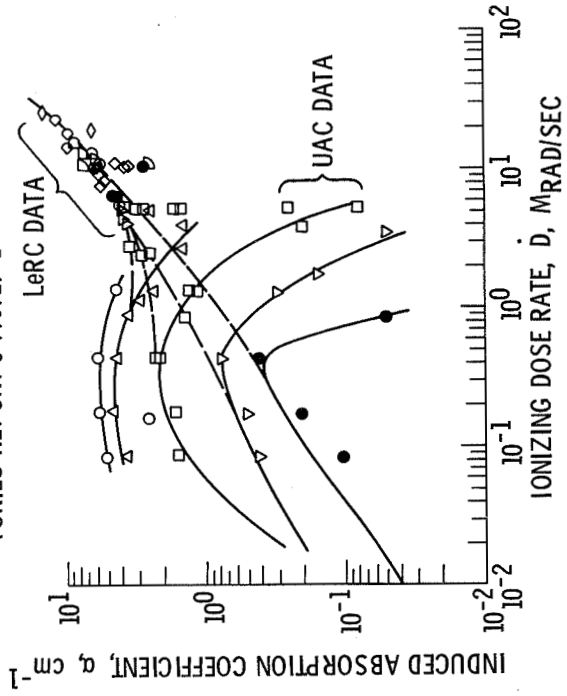
Figure 7. – Steady state induced absorption coefficient at elevated temperatures of specimen during electron irradiation at 2150 Å.

IONIZING DOSE RATE, $\dot{D}$, M$_{RAD}$/SEC

SPECIMEN TEMPERATURE, T, °C

INDUCED ABSORPTION COEFFICIENT, α, cm^{-1}
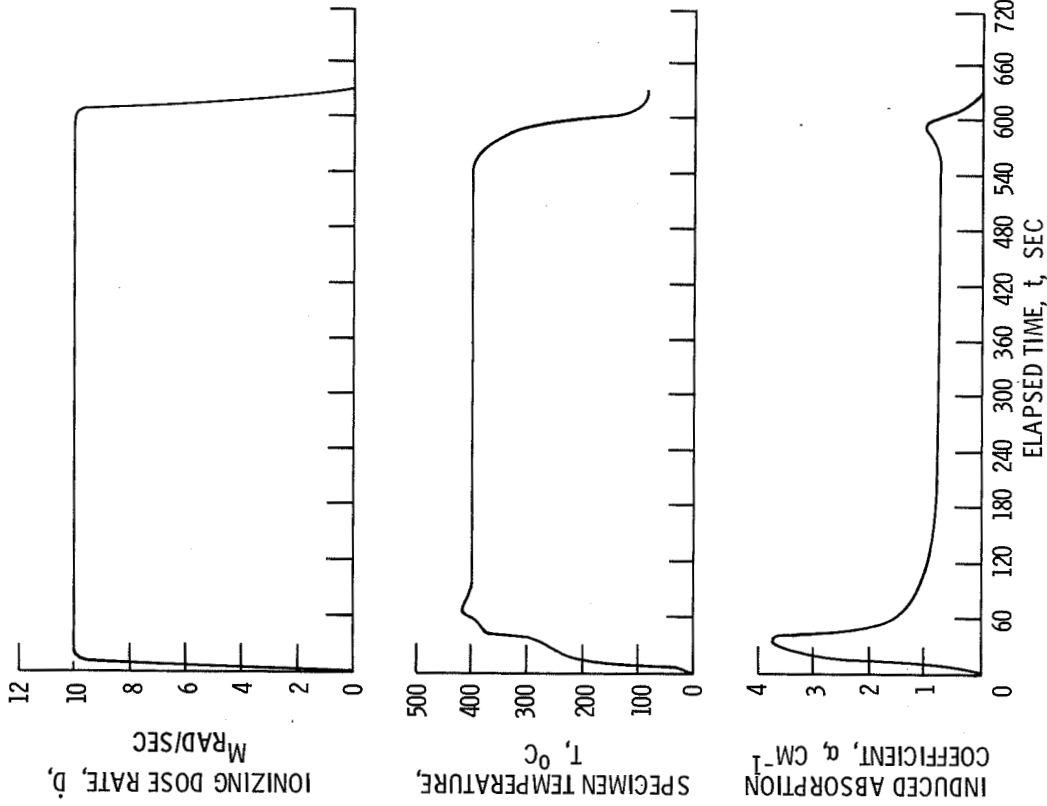
ELAPSED TIME, t, SEC

Figure 6. – Electron irradiation history of 1.5 mm, Suprasil I specimen at 4500 Å.